

CORRODED METAL SHEET FN 655.13.01 – FE ALLOY – MODERN TIMES – SWITZERLAND

Artefact name Corroded metal sheet FN 655.13.01

Authors Marianne. Senn (EMPA, Dübendorf, Zurich, Switzerland) & Christian. Degriigny (HE-Arc CR, Neuchâtel, Neuchâtel, Switzerland)

Url /artefacts/375/

✧ The object

Fig. 1: Iron (and steel) sheet (after Senn Bischofberger 2005, 137),



Credit HE-Arc CR.

✧ Description and visual observation

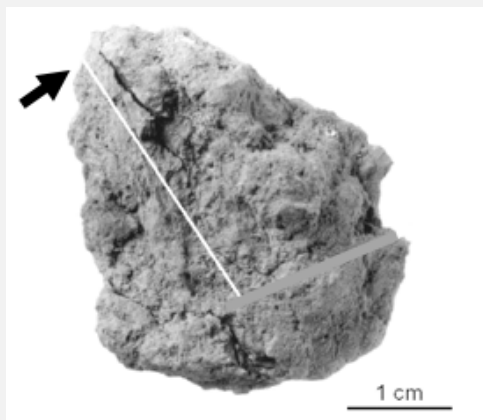
| | |
|----------------------------------------|------------------------------------------------------------------------------------------------------------------------------------------------------------|
| Description of the artefact | Iron sheet with middle rib. The shape is no longer discernible (Fig. 1). The metal is covered by a thick corrosion crust. Dimensions: L = 4.5cm; WT = 35g. |
| Type of artefact | Iron (and steel) sheet |
| Origin | Steinmöri, Neftenbach / Dorf Neftenbach, Zurich, Switzerland |
| Recovering date | Excavation of the Roman villa, 1986-1990, phase S2, StbII.2 (2nd/3rd century AD) |
| Chronology category | Modern Times |
| chronology tpq | <input type="text" value="1986"/> A.D. ▾ |
| chronology taq | <input type="text" value="1990"/> A.D. ▾ |
| Chronology comment | 20th century (1986 _ 1990) |
| Burial conditions / environment | Soil |
| Artefact location | Kantonsarchäologie, Dübendorf, Zurich |
| Owner | Kantonsarchäologie, Dübendorf, Zurich |

Inv. number FN 655.13.01
Recorded conservation data Not conserved

Complementary information

Nothing to report.

Study area(s)



Credit HE-Arc CR.

Fig. 2: Location of sampling area,

Binocular observation and representation of the corrosion structure

Stratigraphic representation: none.

MiCorr stratigraphy(ies) – Bi

Sample(s)

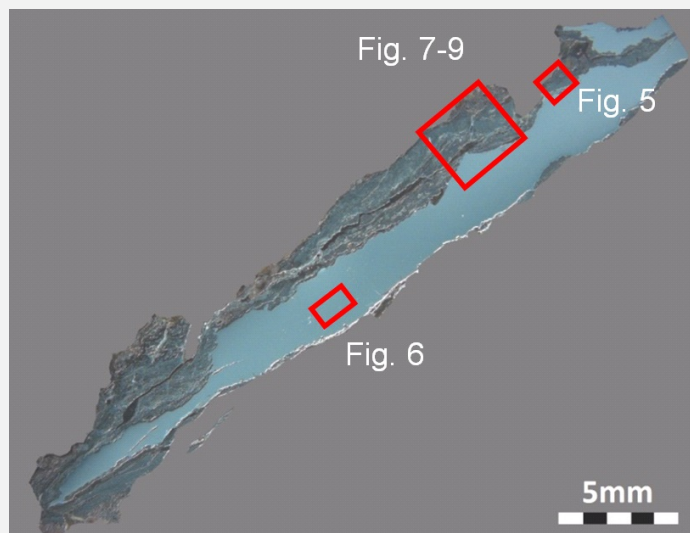


Fig. 3: Micrograph of the cross-section showing the location of Figs. 5 to 9,

| | |
|---------------------------------|------------------------------------------------------------------------------------------------------------------------------------|
| Description of sample | A longitudinal cut has been made through the sheet (Fig. 2). Large parts of the corrosion crust fell off during sampling (Fig. 3). |
| Alloy | Fe Alloy |
| Technology | Forged with final cold work |
| Lab number of sample | NEF 655 |
| Sample location | Empa (Marianne Senn) |
| Responsible institution | Kantonsarchäologie, Dübendorf, Zurich |
| Date and aim of sampling | 2000, metallography |

Complementary information

Nothing to report.

∨ Analyses and results

Analyses performed:

Metallography (nital etched), Vickers hardness testing, LA-ICP-MS, SEM/EDS.

∨ Non invasive analysis

∨ Metal

The remaining metal is an iron containing elevated (more than 1g/kg) concentrations of Co and Ni (Table 1), small round slag inclusions and cracks resulting from corrosion and deformation (Fig. 5). The composition of the round, elongated slag inclusions is similar to wüstite-FeO (Table 2). Iron reduced in the direct smelting process never contains such pure compounds and only FeO inclusions. In modern steels FeO occurs in low carbon alloys and Armco-iron (Schumann 1991, 474). After etching, the cross-section shows a heavily deformed ferritic microstructure from cold working (Fig. 6). The cracks have the same orientation as the deformation. The average hardness of the metal is HV1 195.

| Elements | Al | Ti | V | Cr | Mn | P | Co | Ni | Cu | As | Mo | Ag | Sn | Sb | W | Ni/Co |
|-----------------------|----|----|----|----|----|-----|------|------|-----|-----|----|----|----|----|---|-------|
| Median, mg/kg | < | < | < | < | 20 | 300 | 1100 | 1200 | 800 | 200 | < | < | 60 | 10 | < | 1.1 |
| RSD % | - | - | - | - | 3 | 17 | 6 | 5 | 35 | 15 | 13 | - | 35 | 45 | - | 4 |
| Detection limit mg/kg | 6 | 9 | 19 | 17 | 2 | 77 | 1 | 4 | 2 | 3 | 3 | 1 | 1 | 1 | 3 | - |

Table 1: Chemical composition of the iron. Method of analysis: LA-ICP-MS, Lab of Inorganic Chemistry, ETH.

| Elements | O | Fe | Total |
|-------------------|----|----|-------|
| Round inclusion 1 | 21 | 75 | 96 |
| Round inclusion 2 | 20 | 74 | 95 |

| | | | |
|-------------------|----|----|----|
| Round inclusion 3 | 20 | 75 | 96 |
| Round inclusion 4 | 20 | 73 | 93 |

Table 2: Chemical composition (mass %) of some of the round inclusions of Fig. 5. Method of analysis: SEM/EDS, Laboratory of Analytical Chemistry, Empa.

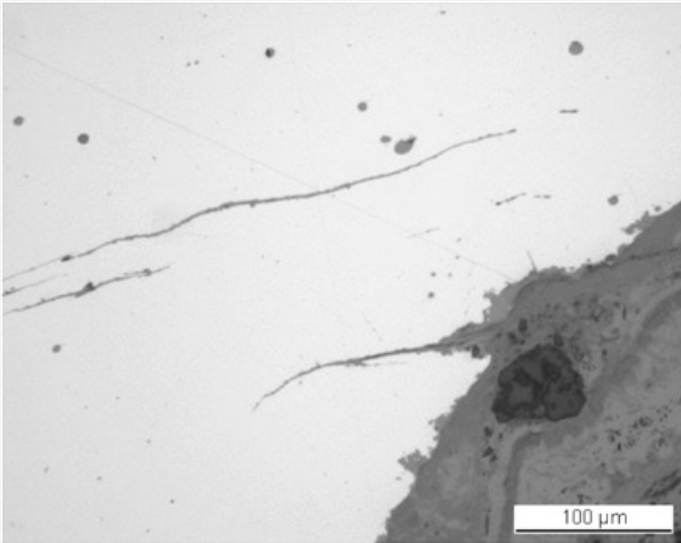


Fig. 5: Micrograph of metal sample from Fig. 3 (inverted picture, detail), unetched, bright field. In white the metal with round slag inclusions as well as cracks filled with corrosion products,

Credit HE-Arc CR.

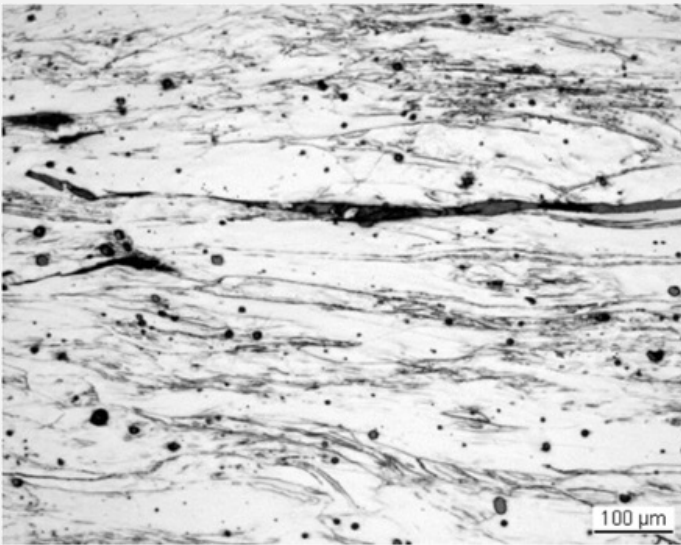


Fig. 6: Micrograph of metal sample from Fig. 3 (detail), etched, bright field. The heavily cold worked metal shows elongated grains with nearly invisible grain boundaries and cracks parallel to the grains,

Credit HE-Arc CR.

| | |
|-----------------------------|------------------------------------------|
| Microstructure | Heavily deformed ferritic microstructure |
| First metal element | Fe |
| Other metal elements | Co, Ni, Cu |

Complementary information

Nothing to report.

✧ Corrosion layers

The corrosion is massive and large parts of the outer corrosion layers have been lost during the sample preparation. The heavily cracked corrosion crust represents about one third of the thickness of the sample (Fig. 3) and is located on one side of the metal

(the rest having been lost during the cutting process). It does not show well defined layers. Despite this, three areas can be distinguished (Figs. 7 and 8). Adhering to the metal (area 1), we find an orange-red-brown layer enriched in Cl (CP3 in Fig. 4, Fig. 9 and Table 3). The dark or violet middle area 2 is richer in Fe (CP2 in Fig. 4). The outer area 3 is red-brown (CP1 in Fig. 4) and strongly contaminated by soil material (rock fragment inclusion and elements like Si, Al, P etc.). This layer is enriched in O (Fig. 9).

| Elements | Location | O | Na | Al | Si | P | Cl | Fe | Cu | Mo | Total |
|--------------|------------------|----|-----|-----|-----|-----|-----|----|-----|-----|-------|
| Area 1 (CP3) | Dark-brown | 31 | < | < | < | < | < | 67 | < | < | 99 |
| | Dark-brown | 35 | < | < | < | < | 0.7 | 64 | < | < | 100 |
| | Red-brown | 38 | < | < | < | < | 2.2 | 64 | < | 0.6 | 104 |
| | Red-brown | 36 | < | < | < | < | 3.3 | 67 | < | < | 106 |
| | Red-brown | 39 | < | < | < | < | 1.3 | 63 | < | < | 104 |
| | Orange-brown | 35 | 1.3 | < | < | < | < | 61 | < | < | 98 |
| Area 2 (CP2) | Orange-brown | 31 | < | < | < | < | 0.7 | 63 | < | < | 95 |
| | Violet-brown | 30 | < | < | < | < | < | 75 | 0.8 | 1.0 | 108 |
| | Brown | 30 | < | < | < | < | < | 77 | < | 0.6 | 108 |
| | Violet-brown | 35 | < | < | < | < | < | 68 | < | < | 103 |
| | Yellow | 33 | < | < | < | < | < | 67 | < | < | 100 |
| | Violet-brown | 32 | < | < | < | < | < | 74 | < | < | 106 |
| Area 3 (CP1) | Quartz inclusion | 54 | < | < | 52 | < | < | < | < | < | 106 |
| | Mixture brown | 42 | < | < | 1.6 | 0.7 | < | 58 | < | < | 102 |
| | Mixture brown | 39 | < | 1.9 | 4.3 | < | < | 56 | < | < | 102 |
| | Mixture brown | 35 | < | < | 0.9 | < | < | 59 | < | < | 95 |

Table 3: Chemical composition (mass %) of the corrosion products from near the metal (area 1, CP3) to the outer surface (area 3, CP1). Method of analysis: SEM/EDS, Laboratory of Analytical Chemistry, Empa.

Corrosion form Uniform - transgranular

Corrosion type ?

Complementary information

Nothing to report.

✧ MiCorr stratigraphy(ies) – CS

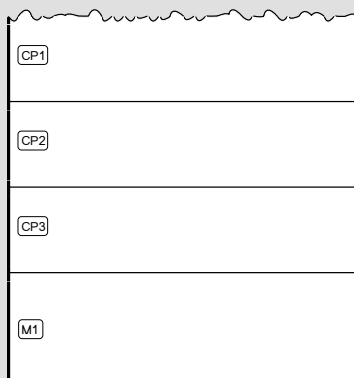


Fig. 4: Stratigraphic representation of the object in cross-section using the MiCorr application. This representation can be compared to Figs. 7 and 8, Credit HE-Arc CR.

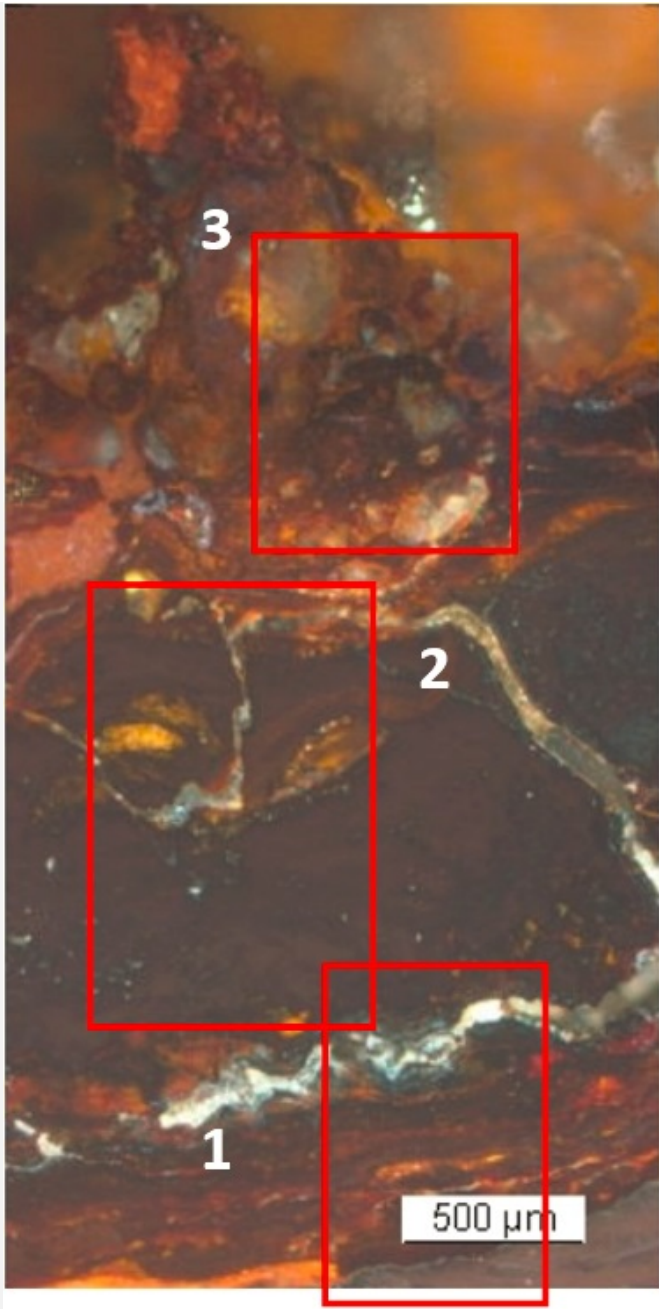
Corrected stratigraphic representation: none.



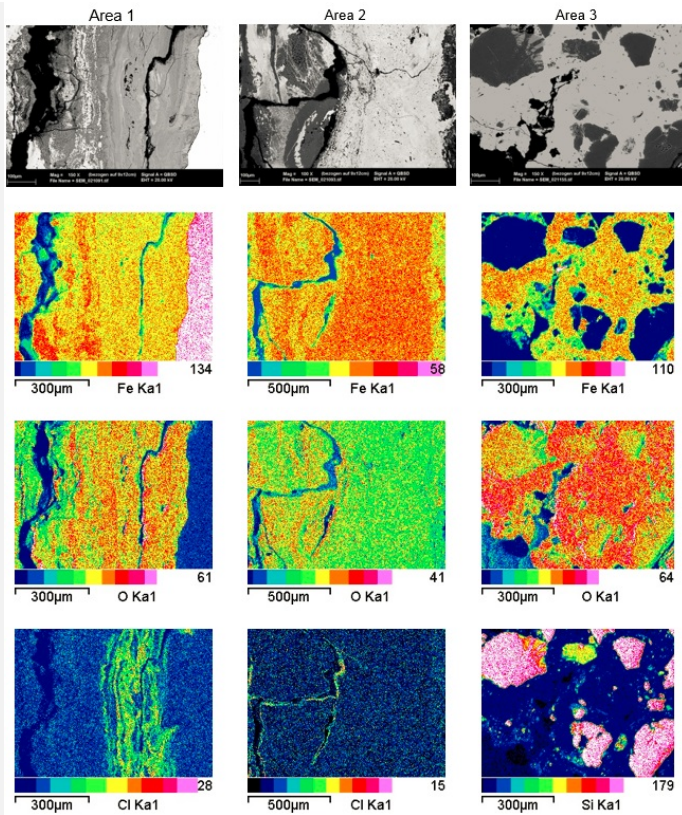
Fig. 7: Micrograph of the corrosion layer from Fig. 3 showing the metal - corrosion crust interface (detail, rotated by 45°) and corresponding to the stratigraphy of Fig. 4, unetched, bright field. Areas 1 (inner layer, CP3) to 3 (outer layer, CP1) are indicated,

Credit HE-Arc CR.

Fig. 8: Micrograph (same as Fig.7) and corresponding to the stratigraphy of Fig. 4, polarised light. The inner layer (CP3) is red-brown, area 2 is brown-violet (CP2) and the outer pale brown area contains rock fragment inclusions (CP1),



Credit HE-Arc CR.



Credit Empa.

Fig. 9: SEM images, BSE-mode, and elemental chemical distribution of the selected areas from Fig. 8 (reversed picture rotated by 270°, details). First column: mapping on area 1 (CP3) where an inner layer enriched in Cl appears near the metal surface. 2nd column: area 2 (CP2) where iron oxides prevail. 3rd column: area 3 (CP1) where the outer O-rich layer includes rock fragments rich in Si. Method of examination: SEM/EDS, Lab. Anal. Chem. Empa,

Conclusion

This iron sheet is entirely cold worked and hard compared to an annealed metal. The corrosion is massive and masks the shape of the object. The presence of Cl adjacent to the metal surface indicates that the corrosion front is potentially active. The very thick top corrosion layers may have slowed down the corrosion. The object was mentioned as being Roman in Senn Bischofberger 2005, however the chemical composition of the slag inclusions shows that it is a product of the 20th century AD which has been accidentally introduced into a Roman layer.

References

References on object and sample

References object

1. Rychener, J. (1999) Der römische Gutshof in Neftenbach. Katalog, Tafeln und Tabellen. Monographien der Kantonsarchäologie Zürich 31/2 (Zürich und Egg), 138.

References sample

2. Senn Bischofberger, M. (2005) Das Schmiedehandwerk im nordalpinen Raum von der Eisenzeit bis ins frühe Mittelalter. Internationale Archäologie, Naturwissenschaft und Technologie Bd. 5, (Rahden/Westf.), 137-138.

References on analytic methods and interpretation

3. Schumann, H. (1991) Metallographie. Leipzig.